# Beam response to rf-generator noise in the presence of higher-harmonic passive cavities

M. Venturini

*Lawrence Berkeley National Laboratory, University of California, Berkeley, California 94720, USA*

(Received 13 February 2022; accepted 11 May 2022; published 23 May 2022)

We examine the effect of higher-harmonic passive cavities (HHCs) on the beam response to rf noise. Upon invoking certain assumptions to make the problem tractable, we employ Vlasov methods to show that when the dipole approximation applies the HHCs have a generally limited impact. Beam loading in the main cavity is included in the analysis. We illustrate our results and the limitations of our model in application to the Lawrence Berkeley National Laboratory ALS (Advanced Light Source) and the future ALS Upgrade (ALS-U) offering validation against macroparticle simulations.

DOI: 10.1103/PhysRevAccelBeams.25.054404

## I. INTRODUCTION

Higher harmonic rf cavities (HHCs) are often employed in storage rings for bunch lengthening or other purposes [1–9]. Although the impact on collective instabilities has been extensively studied [10–21], not as much attention has been devoted to their effect on the beam response to external perturbations and in particular rf noise [22–24]. Because in typical applications, HHCs work by reducing the restoring force responsible for the longitudinal oscillations, hence reducing the incoherent synchrotron tune, one would intuitively expect that the HHC should enhance the beam response to low-frequency noise. In fact, this is not generally the case.

The conventional approach to the problem [25,26] is not applicable when the single-particle motion is highly nonlinear, the regime in which HHCs are preferably operated, and one has to resort to Vlasov methods [10–13]. These are not very well suited to treat the problem in its full generality but they provide valuable insight when applied to specific cases and under certain approximations. Here we focus on high-energy electron storage rings with a double-frequency rf system consisting of a main and a passive higher-harmonic cavity, with the latter tuned for nearly perfect flattening of the total rf voltage. In the presence of a uniformly filled beam and in the regime where the total rf potential is dominated by the quartic term, the single-particle motion admits an approximate description, which is simple enough to permit a derivation of the solution of the linearized Vlasov equation in analytical form. We use this solution to study the coupled-bunch mode-zero beam response in the dipole approximation to a time-dependent perturbation of the generator phase. A full account of beam loading in the main cavity is a defining aspect of this study.

The main result is the analytical expression for the beam response function found in Sec. IV. The preceding Secs. II and III, and related Appendixes, review the essential features of beam loading and present a derivation of the beam response function in the single-particle linear regime (i.e., without HHC); these results are well known but they are reported in some detail for completeness and to ease the introduction of the Vlasov equation. Finally, in Sec. V, we illustrate the significance of our findings with numerical examples inspired by Advanced Light Source (ALS) and its future upgrade.

## II. EXPRESSIONS FOR THE CAVITIES' VOLTAGE

### A. Main cavity

Following the standard approach, we model the main cavity as an equivalent *RLC*-circuit consisting of two ac current generators (external rf generator and circulating beam current) connected in parallel to a load [27–29]. The load has the cavity fundamental mode impedance, characterized by the loaded shunt impedance $R_{L1}$ and quality factor $Q_{L1}$. Written as a function of the time-of-flight coordinate $\tau$ relative to the synchronous particle, the combined voltage is a sinusoidal wave with peak amplitude $V$ and synchronous phase $\psi_s$

$$\begin{aligned}\mathcal{V}_{\rm main}(\tau) &= V\cos(\omega_{\rm rf}\tau+\psi_s)\\ &= V_g\cos(\omega_{\rm rf}\tau+\psi_{s,g})-V_b\cos(\omega_{\rm rf}\tau-\phi_{r1}-\Phi_1),\end{aligned} \tag{1}$$

where $V_g$ and $V_b$ are the external-generator and beam-loading peak voltages

$$V_g \equiv I_g R_{L1} \cos\phi_{r1}, \tag{2}$$

$$V_b \equiv 2 I_{\rm avg} R_{L1} F_1 \cos\phi_{r1}. \tag{3}$$

The detuning angle $\phi_{r1}$ measures the difference between the generator frequency $\omega_{\rm rf}$ and the cavity resonance frequency. The model presupposes a uniformly filled beam of identical bunches circulating in a ring with all rf buckets occupied, and hence with average current $I_{\rm avg} = eN\omega_{\rm rf}/2\pi$ ($N$ is the bunch population); $I_g$ is the generator current. The beam-induced voltage depends on amplitude $F_1$ and phase $\Phi_1$ of the complex-number form factor defined as the FT of the bunch profile $\rho(\tau)$ normalized to unity, $\tilde{\rho}(\omega) = \int d\tau\, \rho(\tau) e^{i\omega\tau}$, evaluated at the fundamental harmonic: $F_1 e^{i\Phi_1} = \tilde{\rho}(\omega_{\rm rf})$. Finally, $\psi_{s,g} = \psi_s - \phi_{r1} - \theta_L$ is the generator-voltage synchronous phase. It depends on the loading angle $\theta_L = (\theta_V - \theta_g)$, the difference between the total voltage $\theta_V$ and generator current $\theta_g$ phases relative to the lab time $t$, see Appendix A. For later use, note that taking the derivative and setting $\tau = 0$ in (1) yields

$$V_g \sin\psi_{s,g} = V \sin\psi_s - V_b \sin(\phi_{r1} + \Phi_1). \tag{4}$$

It is an exercise in trigonometry (see e.g., [27,29]) to show that $\theta_L$ depends on the beam loading $Y = 2I_{\rm avg} R_{L1} F_1 / V$ and other parameters as

$$\tan\theta_L = \frac{Y \sin(\psi_s + \Phi_1) - \tan\phi_{r1}}{1 + Y\cos(\psi_s + \Phi_1)}. \tag{5}$$

This formula has significance for machine operation as the required generator power is minimized when $\theta_L = 0$ [27,28], giving the following prescription for the detuning angle $\phi_{r1}$:

$$\tan\phi_{r1} = \frac{2 I_{\rm avg} R_{L1} F_1}{V} \sin(\psi_s + \Phi_1). \tag{6}$$

At equilibrium with $\Phi_1 \simeq 0$ and $\sin\psi_s > 0$ (beam-phase stability) the rhs of the above equation is positive and therefore $\phi_{r1} > 0$.

### B. Passive higher-harmonic rf cavity

Lacking an external generator, the voltage in a passive HHC is entirely due to beam loading. The expression for the voltage is similar to the second term on the rhs of (1):

$$\mathcal{V}_{\rm HHC}(\tau) = -2 I_{\rm avg} R_n F_n \cos\phi_{rn} \cos(n\omega_{\rm rf}\tau - \phi_{rn} - \Phi_n), \tag{7}$$

with the difference that now $R_n$ and $\phi_{rn}$ represent the HHC shunt impedance and detuning angle, and the beam form factor is evaluated at the $n$ harmonic of $\omega_{\rm rf}$: $F_n e^{i\Phi_n} = \tilde{\rho}(n\omega_{\rm rf})$. If there is no coupler, in a passive HHC, the only control parameter is the detuning $\phi_{rn}$. For bunch lengthening, $\phi_{rn}$ is adjusted to flatten the total (main cavity + HHC) voltage. The condition where the slope (first-order derivative) of the HHC voltage cancels off that of the main cavity is approximately (see e.g., [19])

$$\sin 2\phi_{rn} \simeq -\frac{V \sin\psi_s}{I_{\rm avg} n R_n F_n}, \tag{8}$$

implying that $\phi_{rn} < 0$; the approximation stems from ignoring the precise form of the equilibrium and assuming $\Phi_n \simeq 0$.

For a given average beam current, there exists a special value of the shunt impedance $R_n$ such that the second-order derivative of the total voltage also vanishes (assuming a uniform beam fill). With these settings (which following common language we will refer to as "optimal"), the single-particle (i.e., incoherent) synchrotron tune is linear with the oscillation amplitude and the equilibrium bunch form is a very good approximation of a flattop, see Eq. (39), in which case $\Phi_n = 0$. The HHC-modified synchronous phase is $\cos\psi_s = [n^2/(n^2-1)]\cos\psi_{s0}$, where $\cos\psi_{s0}$ is the phase without HHC. (In the following, the notation $\psi_s$ will indicate the appropriate synchronous phase for the system under consideration whether or not it includes the HHC.)

## III. SIMPLE DERIVATION OF THE BEAM RESPONSE (NO HHC)

We start from the single-particle equations of longitudinal motion

$$\frac{d\tau}{dt} = \alpha_c \delta, \tag{9}$$

$$\frac{d\delta}{dt} = \frac{e\mathcal{V}_{\rm main}(\tau) - U_0}{E_0 T_0}, \tag{10}$$

where $\alpha_c > 0$ (ultrarelativistic approximation) is the momentum compaction, $T_0$ is the revolution time, $E_0$ is the design beam energy, $\delta$ is the relative deviation from the design energy, and $e > 0$ is the elementary charge.

We regard the amplitude of the generator phase error $\Delta\theta_g$ as a first-order perturbation and make use of results from Appendix A to do a combined first-order expansion in $\tau$ and $\Delta\theta_g$ of both the generator and beam-loading components of $\mathcal{V}_{\rm main}(\tau)$, see Eqs. (A13) and (A14). With the energy lost by the synchronous particle given by $U_0 = eV\cos\psi_s = V_g \cos\psi_{s,g} - V_b \cos\phi_{r1}$, we can then combine (9) and (10) to obtain

$$\frac{d^2\tau}{dt^2} = -\frac{e\alpha_c\omega_{\rm rf}}{E_0 T_0}\left[\tau V_g \sin\psi_{s,g} + (\tau - \langle\tau\rangle) V_b \sin\phi_{r1} - \frac{\Delta\theta_g}{\omega_{\rm rf}} V_g \sin\psi_{s,g}\right], \tag{11}$$

where $\langle\cdot\rangle$ is the average over the bunch longitudinal density.

Absent noise ($\Delta\theta_g = 0$) and with the beam at equilibrium, the bunch profile is a zero-average Gaussian. Therefore $\langle\tau\rangle = 0$ and the single-particle motion obeys

$$\frac{d^2\tau}{dt^2} = -\frac{e\alpha_c\omega_{\rm rf}}{E_0T_0}[V_g\sin\psi_{s,g} + V_b\sin\phi_{r1}]\tau = -\frac{e\alpha_c\omega_{\rm rf}V\sin\psi_s}{E_0T_0}\tau = -\omega_s^2\tau, \tag{12}$$

where we have made use of (4) with $\Phi_1 = \langle\tau\rangle = 0$ and recognized the expression for the (incoherent) synchrotron tune

$$\omega_s^2 = \frac{e\alpha_c\omega_{\rm rf}V\sin\psi_s}{E_0T_0}. \tag{13}$$

If the beam is not at equilibrium and instead undergoes rigid dipole oscillations driven by a generator-phase perturbation, the beam-centroid equation of motion is obtained by taking the average $\langle\cdot\rangle$ of both sides of (11) over the bunch distribution. By doing so, the second term in the brackets (the beam-loading term) vanishes and therefore

$$\frac{d^2\langle\tau\rangle}{dt^2} = -\frac{e\alpha_c\omega_{\rm rf}V_g\sin\psi_{s,g}}{E_0T_0}\left[\langle\tau\rangle - \frac{\Delta\theta_g}{\omega_{\rm rf}}\right]. \tag{14}$$

We conclude that in contrast to the incoherent tune, the coherent tune

$$\omega_{c1}^2 = \frac{e\alpha_c\omega_{\rm rf}V_g\sin\psi_{s,g}}{E_0T_0} \tag{15}$$

depends on the *generator* voltage-amplitude and synchronous phase rather than the *total* voltage-amplitude and synchronous phase. An alternate expression for $\omega_{c1}$ follows from (2) and (4): with $\Phi_1 = 0$,

$$\omega_{c1}^2 = \frac{e\alpha_c\omega_{\rm rf}}{E_0T_0}[V\sin\psi_s - I_{\rm avg}R_{L1}F_1\sin 2\phi_{r1}] = \omega_s^2\left(1 - I_{\rm avg}R_{L1}F_1\frac{\sin 2\phi_{r1}}{V\sin\psi_s}\right), \tag{16}$$

showing that $\omega_{c1} \le \omega_s$ as in normal operations $\phi_{r1} > 0$. If the condition (6) is satisfied, the coherent tune can be written as $\omega_{c1}^2 = \omega_s^2(1 - Y^2\cos^2\phi_{r1}) = \omega_s^2(\frac{1-Y^2\cos^2\psi_s}{1+Y^2\sin^2\psi_s})$. From Eq. (16), in the requirement that $\omega_{c1}^2$ be positive, we recognize the dc Robinson stability condition

$$I_{\rm avg}R_{L1}F_1\frac{\sin 2\phi_{r1}}{V\sin\psi_s} < 1. \tag{17}$$

Inserting $\gamma_d = \tau_d^{-1} > 0$ to capture radiation damping, the equation of motion (14) becomes

$$\frac{d^2\langle\tau\rangle(t)}{dt^2} + 2\gamma_d\frac{d\langle\tau\rangle(t)}{dt} + \omega_{c1}^2\langle\tau\rangle(t) = \frac{\omega_{c1}^2}{\omega_{\rm rf}}\Delta\theta_g(t), \tag{18}$$

and taking the Fourier transform yields the transfer function $\langle\tilde\tau\rangle(\omega) = -\frac{\omega_{c1}^2}{\omega_{\rm rf}}\frac{\Delta\tilde\theta_g(\omega)}{\omega^2+2i\gamma\omega-\omega_{c1}^2}$. Finally, with $\Delta\tilde\varphi_b(\omega) = \omega_{\rm rf}\langle\tilde\tau\rangle(\omega)$, the generator-phase to beam-phase transfer function is

$$\frac{\Delta\tilde\varphi_b}{\Delta\tilde\theta_g} = -\frac{\omega_{c1}^2}{\omega^2 + 2i\gamma_d\omega - \omega_{c1}^2}. \tag{19}$$

The simple derivation carried out here is incomplete in that it misses the Robinson damping (or possibly antidamping) term associated with beam loading. This term can be recovered by extending the framework of this section (see e.g., [13,25,30,31]); we omit the derivation since that term will appear in Sec. IV A from solving the Vlasov equation.

In linear approximation, the equations of motion (9) and (10) can be regarded as the canonical equations associated with Hamiltonian $\mathcal{H} = \mathcal{H}_0 + \mathcal{H}_g$, where $\mathcal{H}_0 = \frac{\alpha_c}{2}\delta^2 + \frac{\omega_s^2}{2\alpha_c}\tau^2$ and

$$\mathcal{H}_g = -\tau\omega_{c1}^2\Delta\theta_g(t)/(\omega_{\rm rf}\alpha_c). \tag{20}$$

## IV. BEAM RESPONSE DERIVED FROM THE VLASOV EQUATION

The linearized Vlasov equation is solved upon writing the bunch distribution function in the longitudinal phase space as the sum of the equilibrium $f_0(\tau,\delta)$ and a small perturbation $f(\tau,\delta;\omega) = f_0(\tau,\delta) + e^{-i\omega t}f_1(\tau,\delta;\omega)$. We will denote with $\rho_0(\tau)$ and $\rho_1(\tau)$ the associated longitudinal densities. At equilibrium the total voltage is the sum of (1) and (7):

$$\mathcal{V}_0(\tau;\rho_0) = V\cos(\omega_{\rm rf}\tau + \psi_s) - 2I_{\rm avg}R_nF_n\cos\phi_{rn}\cos(n\omega_{\rm rf}\tau - \phi_{rn} - \Phi_n). \tag{21}$$

The notation emphasizes the voltage dependence on the form of the equilibrium $\rho_0$ through the form factor amplitude $F_n$ and phase $\Phi_n$. We assume that the main-cavity parameters are dynamically adjusted to maintain the main-cavity voltage $V$ on target. Upon defining the rf potential

$$\mathcal{U}_0(\tau;\rho_0) = -\int^\tau\frac{e\mathcal{V}_0(\tau';\rho_0) - U_0}{E_0T_0}d\tau', \tag{22}$$

the equilibrium is found by solving the Haissinski equation $\rho_0(\tau) = e^{-\mathcal{U}_0(\tau;\rho_0)/\alpha_c\sigma_\delta^2}/\int e^{-\mathcal{U}_0(\tau';\rho_0)/\alpha_c\sigma_\delta^2}d\tau'$, where $\sigma_\delta$ is the

equilibrium rms energy spread [19,32]. The first-order perturbation to the Hamiltonian for particle motion at equilibrium $\mathcal{H}_0 = \alpha_c\delta^2/2 + \mathcal{U}_0(\tau;\rho_0)$ is

$$\mathcal{H}_1(\tau) = -\int^{\tau} \frac{e\mathcal{V}_1(\tau';\rho_1)}{E_0T_0}d\tau', \tag{23}$$

with $\mathcal{V}_1(\tau;\rho_1) = -I_{\rm avg}\sum_{p=-\infty}^{\infty}\tilde{\rho}_1(p\omega_{\rm rf})Z(p\omega_{\rm rf}+\omega)e^{-ip\omega_{\rm rf}\tau}$, where $Z = Z^{(1)} + Z^{(n)}$ is the sum of the main cavity and HHC fundamental-modes' impedance (Appendix B). Upon introducing the action-angle variables $(J,\varphi)$ and the oscillation frequency $\omega_s(J) = \partial\mathcal{H}_0/\partial J$, we are led to the linearized Vlasov equation in $f_1$:

$$-i\omega f_1 + \omega_s(J)\frac{\partial f_1}{\partial\varphi} - \frac{\partial f_0}{\partial J}\frac{\partial\mathcal{H}_1}{\partial\varphi} = \frac{\partial f_0}{\partial J}\frac{\partial\mathcal{H}_g}{\partial\varphi}. \tag{24}$$

The equation is solved by mode analysis (see Appendix C for the details) under the assumption that the canonical transformation to action-angle variables has the form $\tau = r(J)\cos\varphi$, with the single-particle oscillation amplitude $r(J)$ being a function of the action only. This form captures the two cases of interest in this paper: (i) linear motion (no HHC) and (ii) optimal HHC tuning. It is exact in the first case; approximate but reasonably accurate in the second [11]. Radiation damping is accounted for heuristically by insertion of a mode-dependent term, see Eq. (C1). The rhs term of Eq. (24) involves the external-generator noise term: $\mathcal{H}_g$ is the same as (20) with $\Delta\theta_g(t) = e^{-i\omega t}\Delta\tilde{\theta}_g(\omega)$. In action-angle variables,

$$\frac{\partial\mathcal{H}_g}{\partial\varphi} = \frac{\omega_{c1}^2\Delta\tilde{\theta}_g(\omega)}{\omega_{\rm rf}\alpha_c}r(J)\sin\varphi, \tag{25}$$

with $\omega_{c1}$ as in (16). Once the solution to Eq. (24) is known, the beam-centroid response is calculated as

$$\Delta\tilde{\varphi}_b(\omega) = \omega_{\rm rf}\langle\tilde{\tau}\rangle(\omega) = \omega_{\rm rf}\int\tau f_1(\tau,\delta;\omega)d\tau d\delta, \tag{26}$$

with the final result

$$\frac{\Delta\tilde{\varphi}_b}{\Delta\tilde{\theta}_g} \simeq \frac{\omega_{c1}^2}{\alpha_c}\frac{G_{1,1}}{1 + i\hat{I}[G_{1,1}\zeta_1 + G_{n,n}\zeta_n] + \hat{I}^2[G_{1,1}G_{n,n} - (G_{1,n})^2]\zeta_1\zeta_n} \tag{27}$$

for the beam response function, where

$$\hat{I} = \frac{e\omega_{\rm rf}I_{\rm avg}}{E_0T_0} \tag{28}$$

(units of $\mathrm{Hz}^2/\Omega$) is the scaled beam current parameter;

$$\zeta_1(\omega) = \sum_{p=\pm1} pZ^{(1)}(p\omega_{\rm rf}+\omega), \tag{29}$$

$$\zeta_n(\omega) = \sum_{p=\pm n} pZ^{(n)}(p\omega_{\rm rf}+\omega) \tag{30}$$

are the effective impedances associated with the fundamental modes of the main and harmonic cavity; and the functions $G_{p,q}(\omega)$ are defined in (C13).

### A. No HHC (short-bunch approximation)

In the absence of HHC ($\zeta_n = 0$), the beam response function (27) reduces to

$$\frac{\Delta\tilde{\varphi}_b}{\Delta\tilde{\theta}_g} = \frac{\omega_{c1}^2}{\alpha_c}\frac{1}{\frac{1}{G_{1,1}(\omega)} + i\hat{I}\zeta_1(\omega)}. \tag{31}$$

Because the longitudinal motion in the rf bucket is linear and the synchrotron tune $\omega_s$ is independent of the oscillation amplitude, the evaluation of $G^{1,1}(\omega)$ defined in (C13) is trivial; after expanding the Bessel functions to first order (short-bunch approximation, $\omega_{\rm rf}\sigma_\tau \ll 1$), we have

$$\begin{aligned} G_{1,1} &\simeq \frac{4\pi\omega_s}{\omega^2 + 2i\gamma_d\omega - \omega_s^2}\int_0^\infty\frac{\partial f_0}{\partial J}\frac{r^2}{4}dJ \\ &= -\frac{\alpha_c}{\omega^2 + 2i\gamma_d\omega - \omega_s^2}, \end{aligned} \tag{32}$$

since $2\pi\int_0^\infty dJ f_0(J) = 1$ and for linear motion $r = \sqrt{2J\alpha_c/\omega_s}$. Expanding the main-cavity effective impedance through first order is generally a good approximation, so that $\zeta_1(\omega) \simeq \zeta_1(0) + \zeta_1'(0)\omega$ with $\zeta_1(0)$ and $\zeta_1'(0)$ given in (B5) and (B7), Eq. (31) becomes

$$\frac{\Delta\tilde{\varphi}_b}{\Delta\tilde{\theta}_g} = -\frac{\omega_{c1}^2}{\omega^2 + 2i\omega[\gamma_d - \alpha_c\frac{\hat{I}}{2}\zeta_1'(0)] - [\omega_s^2 + i\alpha_c\hat{I}\zeta_1(0)]}. \tag{33}$$

Inspection of the denominator leads to the following identification of the coherent mode frequency $\omega_c$ and Robinson damping rate $\gamma_R$:

$$\omega_c^2 = \omega_s^2 + i\alpha_c\hat{I}\zeta_1(0) = \omega_s^2 + (\omega_{c1}^2 - \omega_s^2) = \omega_{c1}^2 \tag{34}$$

$$\gamma_R = -\frac{1}{2}\alpha_c\hat{I}\zeta_1'(0) = 2\frac{e\alpha_cI_{\rm avg}}{E_0T_0}R_{L1}Q_{L1}\sin 2\phi_{r1}\cos^2\phi_{r1}. \tag{35}$$

In (34), we made use of (16) with $F_1 \simeq 1$ and the definitions (28) and (B5) for the current parameter $\hat{I}$ and $\zeta_1(0)$ to write

$$i\alpha_c\hat{I}\zeta_1(0) = \alpha_c\hat{I}R_{L1}\sin 2\phi_{r1} = \frac{e\alpha_c\omega_{\rm rf}I_{\rm avg}}{E_0T_0}R_{L1}\sin 2\phi_{r1} = \frac{e\alpha_c\omega_{\rm rf}V\sin\psi_s}{E_0T_0}\frac{I_{\rm avg}R_{L1}\sin 2\phi_{r1}}{V\sin\psi_s} = \omega_s^2 - \omega_{c1}^2. \tag{36}$$

The third equality above follows from multiplying the numerator and denominator by $V\sin\psi_s$. In conclusion, we have recovered the expression (19) for the beam response function but adjusted to have $\gamma_{\rm tot} = \gamma_d + \gamma_R$ in place of $\gamma_d$, thus now accounting for Robinson damping.

### B. HHC with optimum tuning

With optimum HHC settings, the rf total potential is dominated by the quartic term $\propto \tau^4$ and the canonical transformation from action angle to the longitudinal coordinate is approximately $\tau \simeq r(J)\cos\varphi$, where $r(J) = [\sqrt{\pi}\sigma_\tau^2 J/(\sqrt{2}\sigma_\delta)]^{1/3}$ [11]. The quantities relevant in the calculation include the single-particle oscillation frequency $\omega_s(r)$, a function linear in $r$, the average oscillation frequency $\langle\omega_s\rangle = \int d\varphi \int dJ f_0(J)\omega_s(J)$ within a bunch at equilibrium, and the equilibrium $f_0$:

$$\omega_s(r) = \frac{2^{3/4}\pi^{3/2}}{\Gamma^2(1/4)}\langle\omega_s\rangle\frac{r}{\sigma_\tau} \simeq 0.712\times\langle\omega_s\rangle\frac{r}{\sigma_\tau}, \tag{37}$$

$$\langle\omega_s\rangle = \frac{2\times 2^{3/4}\pi}{\Gamma^2(1/4)}\frac{\alpha_c\sigma_\delta}{\sigma_\tau} \simeq 0.803\times\frac{\alpha_c\sigma_\delta}{\sigma_\tau}, \tag{38}$$

$$f_0(r) = \frac{2^{3/4}}{\Gamma^2(1/4)\sigma_\tau\sigma_\delta}e^{-2\pi^2r^4/[\Gamma^4(1/4)\sigma_\tau^4]}, \tag{39}$$

where $\Gamma(1/4) \simeq 3.62$ is the Euler function. All these quantities are expressed in terms of the optimum equilibrium rms bunch length $\sigma_\tau$

$$\sigma_\tau^2 = \sigma_\delta\frac{4\pi\sqrt{3}/\Gamma^2(1/4)}{\sqrt{(n^2-1)}}\sqrt{\frac{\alpha_cE_0T_0}{eV\omega_{\rm rf}^3\sin\psi_s}}. \tag{40}$$

With the above formulas in hand, the functions $G_{p,q}(\omega)$ introduced in (C13) can be written as

$$G_{p,q} = -\frac{4\pi}{\omega_{\rm rf}^2pq}\int_0^\infty\frac{\partial f_0}{\partial r}\frac{\omega_s(r)J_1(p\omega_{\rm rf}r)J_1(q\omega_{\rm rf}r)dr}{\omega^2+2i\gamma_d\omega-\omega_s^2(r)} = -\frac{16\times 2^{1/4}}{pq\Gamma(1/4)\omega_{\rm rf}^2\langle\omega_s\rangle\sigma_\delta\sigma_\tau}\times\int_0^\infty dxe^{-x^4}\frac{x^4J_1(pc_2\omega_{\rm rf}\sigma_\tau x)J_1(qc_2\omega_{\rm rf}\sigma_\tau x)}{\hat{\omega}^2+2i\hat{\gamma}_d\hat{\omega}-x^2}, \tag{41}$$

where $\hat{\omega} = c_1\omega/\langle\omega_s\rangle$ and $\hat{\gamma}_d = c_1\gamma_d/\langle\omega_s\rangle$ are the scaled (and dimensionless) frequency and radiation damping rate with numerical coefficients $c_1 = \frac{\Gamma(1/4)}{\sqrt{2\pi}} \simeq 0.816$ and $c_2 = \frac{\Gamma(1/4)}{2^{1/4}\sqrt{\pi}} \simeq 1.72$. Because radiation damping is included ($\hat{\gamma}_d > 0$) and the $\hat{\omega}$'s of interest are real numbers, the $x$ integral is properly defined along the entire positive real axis.

The response function (27), with $G_{p,q}$ as in (41), is not particularly revealing without resorting to a numerical calculation, see Sec. V. It is instructive to consider the $|\hat{\omega}| \gg 1$ limit in the approximation where the Bessel functions in (41) are expanded to first order, although typically this approximation applied to $G_{n,n}$ tends not to be very accurate. Nevertheless, taking this limit $\int_0^\infty dxe^{-x^4}x^4J_1(pc_2\omega_{\rm rf}\sigma_\tau x)\times J_1(qc_2\omega_{\rm rf}\sigma_\tau x) \simeq (3/64)\Gamma(1/4)\times pq\omega_{\rm rf}^2\sigma_\tau^2$, and we find

$$G_{1,1} \simeq G_{n,n} \simeq -\frac{g_{11}\alpha_c}{\omega^2+2i\gamma_d\omega}, \tag{42}$$

with numerical coefficient $g_{11} = \frac{6\pi^3}{\Gamma^4(1/4)} \simeq 1.08$. Equation (27) becomes

$$\frac{\Delta\tilde{\varphi}_b}{\Delta\tilde{\theta}_g} \simeq \frac{g_{11}\omega_{c1}^2}{\omega^2+2i\gamma_d\omega-i\alpha_cg_{11}\hat{I}\zeta(\omega)} \simeq \frac{g_{11}\omega_{c1}^2}{\omega^2+2i\omega[\gamma_d-\alpha_cg_{11}\frac{\hat{I}}{2}\zeta'(0)]-i[\alpha_cg_{11}\hat{I}\zeta(0)]}, \tag{43}$$

where we expanded the total effective impedance $\zeta(\omega) = \zeta_1(\omega)+\zeta_n(\omega)$ through the first order in $\omega$. Inspecting the denominator, we can read off the coherent-mode oscillation frequency $\omega_c$ and Robinson damping $\gamma_R$:

$$\omega_c^2 \simeq i\alpha_cg_{11}\hat{I}\zeta(0) = g_{11}\left[\omega_{c1}^2+\left(\frac{1}{F_n}-1\right)\omega_s^2\right], \tag{44}$$

$$\gamma_R \simeq -\frac{1}{2}\alpha_cg_{11}\hat{I}\zeta'(0) = 2g_{11}\frac{e\alpha_cI_{\rm avg}}{E_0T_0}(R_{L1}Q_{L1}\sin 2\phi_{r1}\cos^2\phi_{r1} + R_nQ_n\sin 2\phi_{rn}\cos^2\phi_{rn}), \tag{45}$$

having used

$$i\alpha_c\hat{I}\zeta_1(0) = i\alpha_c\hat{I}R_{L1}\sin 2\phi_{r1} = \frac{e\alpha_c\omega_{\rm rf}I_{\rm avg}}{E_0T_0}R_{L1}\sin 2\phi_{r1} = \omega_s^2-\omega_{c1}^2, \tag{46}$$

$$i\alpha_c\hat{I}\zeta_n(0) = \alpha_c\hat{I}nR_n\sin 2\phi_{rn} = \frac{e\alpha_c\omega_{\rm rf}I_{\rm avg}}{E_0T_0}nR_n\sin 2\phi_{rn} = \frac{e\alpha_c\omega_{\rm rf}V\sin\psi_s}{E_0T_0}\frac{I_{\rm avg}nR_n\sin 2\phi_{rn}}{V\sin\psi_s} = -\frac{\omega_s^2}{F_n}. \tag{47}$$

Equation (46) is similar to (36). The last equality in (47) follows from (8). Here $\omega_s$ and $\omega_{c1}$ represent the incoherent and coherent tunes that would be observed in a similar storage ring without HHC if synchronous phase $\psi_s$ and detuning $\phi_{r1}$ were the same as when the HHC is present. With reference to Eq. (44), for light sources, a typical value for the form-factor amplitude is about $F_n \simeq 0.9$ implying that $1/F_n - 1$ is a small number. In the particular case where $\omega_{c1} \simeq \omega_{s1}$ and recalling $g_{11} \simeq 1.08$, Eq. (44) is consistent with $\omega_c$ being within about 10% of $\omega_{c1}$. Numerical studies based on the more accurate formula indicate that, for typical machine parameters, the difference tends to be smaller.

## V. NUMERICAL EXAMPLES

### A. The ALS

We discuss two examples. The first, based on ALS, is meant to provide a confirmation of our model; the second, based on the ALS-U [33], to highlight its limitations. The relevant parameters of the two machines are reported in Table I.

The ALS has currently three normal-conducting, third-harmonic single-cell cavities for a total $R_s = 5.1$ MΩ impedance not far from $R_s = 5.9$ MΩ, the optimum shunt impedance for the nominal 500 mA current. The optimum (rms) bunch length is just below $\sigma_z = 17$ mm. Because the ALS operates with a single but relatively long (10%) gap in the beam fill, transient beam-loading effects are strong enough to prevent the attainment of the theoretical bunch lengthening [34]. For the purpose of this exercise, the ideal uniform-fill operational scenario is assumed.

The theory predicts that the beam response with and without HHCs is very close, a result confirmed by macroparticle simulations with ELEGANT [35], see Fig. 1 (left images). The simulations were carried out using ELEGANT's "pseudo-mode" functionality, which effectively allows one to model a uniformly populated multibunch beam by tracking only particles in a single bunch. This is adequate for studying the mode-zero multibunch collective motion. Tracking was done with 10k particles/bunch over about 100k turns with a user-defined sinusoidal perturbation applied to the main-cavity generator phase.

The response function was calculated based on the beam-centroid output recorded at every turn by carrying out a simple discrete Fourier transform (DFT). We found that even with the allowance of enough time for the initial transients to die off, the DFT result showed sensitivity to the choice of the exact range number of turns. Therefore we repeated the DFT using varying length data records between 20k and 100k turns. The data points (error bars) in the figures represent the average response (rms spread). In the simulations, the HHC tuning was set so as to yield the "optimum" bunch length.

### B. The ALS-U

The longitudinal dynamics of the ALS-U will be notably different from that of the ALS. The lower main rf cavity voltage (0.6 vs 1.2 MV) and momentum compaction ($2 \times 10^{-4}$ vs $9 \times 10^{-4}$) will result in a markedly lower incoherent synchrotron tune. The present project goal is to maintain the existing two main rf cavities. The $\beta \simeq 3$ coupling coefficient of these cavities is low compared to

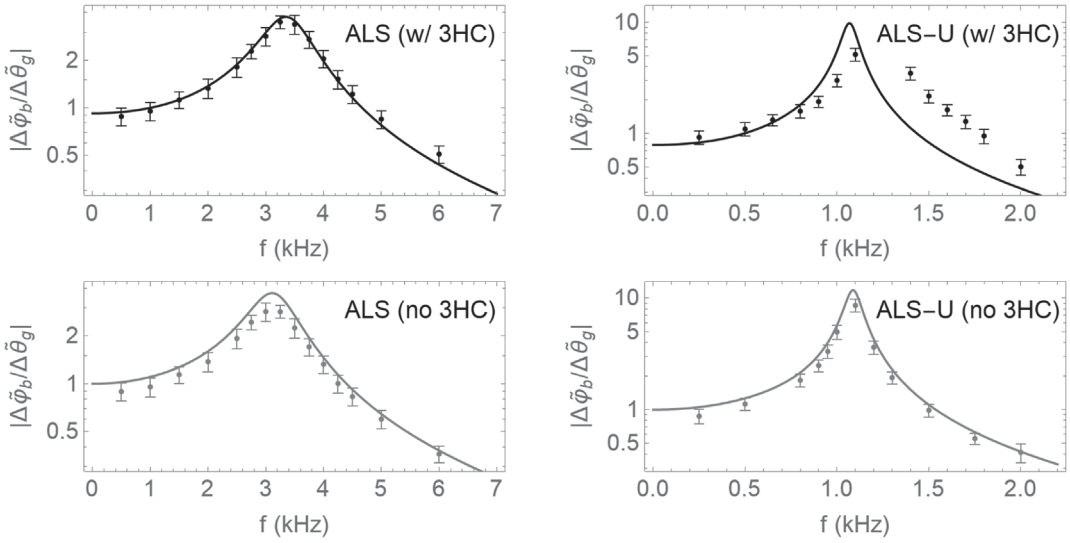


FIG. 1. Amplitude of the beam-centroid response to a sinusoidal perturbation of the rf generator phase with frequency $f = \omega/2\pi$, in the presence (top) and absence (bottom) of higher-harmonic passive cavities as calculated by macroparticle simulations (dots) and theory (curves). The curves with/without 3HCs are from Eq. (27) [with the functions $G_{p,q}$ defined in (41)] and (33), respectively. The peak frequency response is higher and the peak amplitude is lower in the ALS (left) compared to the ALS-U (right). Note the difference in scale in both the horizontal and vertical axes.

TABLE I. Relevant ALS-U and ALS parameters.

| | ALS-U | ALS |
|---|---|---|
| Beam energy, $E_0$ | 2.0 GeV | 1.9 GeV |
| Circumference, $C_0$ | 196.5 m | 196.8 m |
| Average beam current, $I_{\mathrm{avg}}$ | 500 mA | 500 mA |
| Momentum compaction, $\alpha_c$ | $2.03 \times 10^{-4}$ | $0.9 \times 10^{-3}$ |
| Energy loss/turn, $U_0$ | (w/IDs) 0.314 MeV | (no IDs) 0.228 MeV |
| Synchronous phase without/with HHC, $\psi_s$ | 58.37/53.84 deg | 79.04/77.66 deg |
| Energy relative spread, $\sigma_\delta$ | $1 \times 10^{-3}$ | $9.6 \times 10^{-4}$ |
| Longitudinal radiation damping time, $\tau_d$ | 7.8 ms | 5.0 ms |
| Natural bunch length (no HHC), $\sigma_{z0}/\sigma_{\tau 0}$ | 3.93 mm/13.1 ps | 5.01 mm/16.7 ps |
| Stretched bunch length (with HHC), $\sigma_z/\sigma_\tau$ | 15.0 mm/50.0 ps | 16.7 mm/55.9 ps |
| Harmonic number $h$ | 328 | 328 |
| Generator rf frequency, $\omega_{\mathrm{rf}}$ | 500.394 MHz | 499.654 MHz |
| Main-cavity voltage, $V$ | 0.6 MV | 1.2 MV |
| Main-cavity loaded coupling factor, $\beta$ | 10.64 | 2.75 |
| Main-cavity loaded $R_{L1}/Q_{L1}$, | 0.8422 MΩ/3,094 | 2.616 MΩ/9,611 |
| Main-cavity detuning (no HHC), $\phi_{r1}/f_{r1}$ | 50 deg /96 kHz | 64.9 deg /55.6 kHz |
| Main-cavity detuning (with HHC), $\phi_{r1}/f_{r1}$ | 49 deg /91 kHz | 64.5 deg /54.5 kHz |
| Beam-loading parameter, $Y$ | 1.40 | 2.18 |
| HHC higher-harmonic number, $n$ | 3 | 3 |
| HHC $R_n/Q_n$ | 1.4 MΩ/34,000 | 5.1 MΩ/21,000 |
| HHC detuning angle/frequency $\phi_{rn}/f_{rn}$ | −82.4 deg /−165 kHz | −85.1 deg /−416 kHz |
| Synchronous frequency (no HHC), $\omega_s/2\pi$ | 2.5 kHz | 8.22 kHz |
| Synchrotron tune (no HHC), $\nu_s = \omega_s/\omega_0$ | 0.0016 | 0.0054 |
| Average synchronous frequency (with HHC), $\langle\omega_s\rangle/2\pi$ | 0.54 kHz | 2.98 kHz |
| Robinson damping time (no HHC), $\tau_R$ | 6.2 ms | 0.40 ms |
| Robinson nominal damping time (with HHC), $\tau_R$ | 7.1 ms | 0.41 ms |

the ALS-U optimum ($\beta \simeq 10$) and a coupler modification will be made to increase $\beta$. Here we assume optimum $\beta$.

The ALS-U is being designed with two single-cell third-harmonic cavities for a total $R_s = 1.4$ MΩ, somewhat larger than the $R_s = 0.76$ MΩ optimum [36]. Extensive simulations of the ALS-U indicate that with the 3HCs tuned to yield the optimum bunch length ($\sigma_\tau \simeq 15$ mm), the beam exhibits an ac Robinson-like instability with the signature of dipole-quadrupole coupling. Simulations also show that the instability, which saturates to persistent bunch-centroid and length oscillations, can be suppressed with a conventional bunch-by-bunch longitudinal feedback (LFB) system but the LFB is not included in the results reported here. The simulated beam response to a main-cavity generator-phase sinusoidal perturbation is shown in the Fig. 1 top-right image and, as expected, differs somewhat from the theory in the dipole approximation. The simulations indicate a resonant peak at about 1.3 kHz, while the theory places the dipole coherent motion frequency just above 1 kHz. (In the picture we do not report the simulated response close to the peak because the occurring instability interferes with the response beyond linear theory.)

In the absence of harmonic cavities, the simulated response follows the expected behavior (bottom-right image): No instability is observed in this case, implying that the coupled dipole/quadrupole instability is indeed caused by the 3HC. The comparison with the ALS response suggests that ALS-U is potentially more sensitive to rf noise: because of the lower resonant frequency (the rf noise scales with some inverse power of frequency) and because of the higher peak response. Either reason, though, is essentially neutral to the presence of HHC, depending on the lattice and main-cavity parameters (specifically, the lower peak value in the ALS response is due to the larger Robinson damping contributed by the main cavity).

## VI. CONCLUSIONS

The main conclusion to be drawn from this study is the realization of the limited role that passive higher-harmonic cavities play in determining the beam response when the dipole approximation applies.

In general, the beam-response function has the characteristics of a resonance, with peak frequency and peak amplitude related to the real and imaginary parts of the complex eigenfrequency of the system coherent mode(s). Mathematically, the singularities of the response function in the complex-$\omega$ plane are the roots of the dispersion equation that identify the coherent modes' eigenfrequencies. As it turns out, the real part of the dipole-motion eigen-frequency is largely determined by the main-cavity parameters, and specifically the external generator synchronous phase and voltage.

At first it may seem surprising that the presence of passive HHCs, which affect significantly the single-particle motion, should not have a more visible impact on the coherent motion of a bunch as a whole, an observation already made, e.g., in [24]. But this is not unlike dipole motion in other contexts. For example, coherent transverse betatron oscillations in the presence of (direct) space charge are entirely dependent on the external focusing, not interparticle forces. Where HHCs can potentially have a more noticeable role is in the modification of Robinson damping, with a consequence on the response peak amplitude rather than its frequency. The effect is dependent on the system specific parameters. In both the examples discussed here, the Robinson antidamping contributed by the HHC happens to be modest compared to the Robinson damping from the main cavity and radiation damping.

We qualify these conclusions by emphasizing their validity in the dipole approximation. HHCs can, however, induce significant dipole/quadrupole coupling (see [16,24] and the ALS-U example in Sec. V) with the effect of a more noticeable modification of the beam-response resonant frequency. There is no conceptual difficulty in writing an extended beam-response theory to include dipole/quadrupole coupling (this with an account of a longitudinal feedback system will be reported elsewhere; elements of this theory are already in Refs. [11,13,16,24]). Less obvious is how the formalism can be generalized to include the "overstretching" regime, where the HHC tuning is set to the point where the total rf potential develops a double well and conventional perturbation theory does not apply. This generalization would be of interest since it would apply to a regime where simulations indicate that the dipole/quadrupole coupling becomes more prevalent.

## ACKNOWLEDGMENTS

Discussions and support from the members of the LBNL ALS accelerator-physics group and ALS-U project are gratefully acknowledged. This work was supported by the Director of the Office of Science of the U.S. Department of Energy under Contract No. DEAC02-05CH11231.

## APPENDIX A: MAIN-CAVITY TOTAL VOLTAGE

A uniformly filled electron beam consisting of identical bunches with population $N$ and profile $\rho(\tau)$ concentrated at $\tau \simeq 0$ and observed at the cavity has instantaneous current

$$\mathcal{I}(t) = -eN \sum_{m=-\infty}^{\infty} \rho(t - mT_{\rm rf} - t_0). \tag{A1}$$

Interacting with the cavity fundamental mode associated with the wake function $W$ (see Appendix B), the beam induces the voltage $\mathcal{V}_b(t) = \int \mathcal{I}(t')W(t-t')dt'$. In the frequency domain, upon changing the integration variable from $t'$ to $\tau' = t' - mT_{\rm rf} - t_0$,

$$\begin{aligned}\mathcal{V}_b(t) &= -\frac{eN}{2\pi}\int d\omega Z(\omega)\int dt'\rho(t' - mT_{\rm rf} - t_0)e^{-i\omega(t-t')} \\ &= -\frac{eN}{2\pi}\sum_{m=-\infty}^{\infty}\int d\omega Z(\omega)e^{-i\omega t}e^{i\omega m T_{\rm rf}}e^{i\omega t_0} \\ &\quad\times\int d\tau'\rho(\tau')e^{i\omega\tau'}.\end{aligned} \tag{A2}$$

Introducing the Fourier transform $\tilde{\rho}(\omega) = \int d\tau\rho(\tau)e^{i\omega\tau}$ and the Poisson sum formula $\sum_{m=-\infty}^{\infty} e^{i\omega m T_{\rm rf}} = 2\pi\sum_{p=-\infty}^{\infty}\delta(\omega T_{\rm rf} - 2\pi p)$, we find

$$\begin{aligned}\mathcal{V}_b(t) &= -eN\sum_{p=-\infty}^{\infty}\int d\omega\delta(\omega T_{\rm rf} - 2\pi p)Z(\omega)\tilde{\rho}(\omega)e^{-i\omega(t-t_0)} \\ &= -\frac{eN}{T_{\rm rf}}\sum_{p=-\infty}^{\infty}Z(\omega_{\rm rf}p)\tilde{\rho}(\omega_{\rm rf}p)e^{-i\omega_{\rm rf}p(t-t_0)}.\end{aligned} \tag{A3}$$

Assume that the impedance of the main-cavity fundamental mode is sufficiently narrow band and only the $p = \pm 1$ terms contribute to the sum, we conclude ($I_{\rm avg} = eN/T_{\rm rf}$):

$$\begin{aligned}\mathcal{V}_b(t) &\simeq -I_{\rm avg}Z(\omega_{\rm rf})\tilde{\rho}(\omega_{\rm rf})e^{-i\omega_{\rm rf}(t-t_0)} + \text{c.c.} \\ &= -2I_{\rm avg}R_sF_1\cos\phi_{r1}\cos(\omega_{\rm rf}t - \phi_{r1} - \Phi_1 - \omega_{\rm rf}t_0),\end{aligned} \tag{A4}$$

where we have made use of (B1) and (B4) to write $Z(\omega_{\rm rf}) = R_s\cos\phi_{r1}e^{i\phi_{r1}}$ and introduced the amplitude $F_1$ and phase $\Phi_1$ of the bunch complex-number form-factor

$$F_1e^{i\Phi_1} \equiv \tilde{\rho}(\omega_{\rm rf}). \tag{A5}$$

For a short bunch $\tilde{\rho}(\omega_{\rm rf}) \simeq \int d\tau(1 + i\omega_{\rm rf}\tau - \omega_{\rm rf}^2\tau^2/2)\rho(\tau) = 1 - \omega_{\rm rf}^2\langle\tau^2\rangle/2 + i\omega_{\rm rf}\langle\tau\rangle$, and therefore $F_1 \simeq 1 - \omega_{\rm rf}^2\sigma_\tau^2/2$ and

$$\Phi_1 \simeq \omega_{\rm rf}\langle\tau\rangle. \tag{A6}$$

Equation (A4) can be cast in the phasor notation as

$$\mathcal{V}_b(t) = \text{Re}\{e^{-i\omega_{\rm rf}t}\tilde{V}_b\}, \tag{A7}$$

with beam-voltage phasor $\tilde{V}_b = Z(\omega_{\rm rf})\tilde{I}_b$ and beam-current phasor $\tilde{I}_b = -2I_{\rm avg}F_1e^{i\Phi_1}e^{i\omega_{\rm rf}t_0}$. Similarly, phasors can be used to represent the generator and total voltages

$$\mathcal{V}_g(t) = \text{Re}\{e^{-i\omega_{\rm rf}t}\tilde{V}_g\} = I_gR_{L1}\cos\phi_{r1}\cos(\omega_{\rm rf}t - \phi_{r1} + \theta_g), \tag{A8}$$

$$\mathcal{V}(t) = \text{Re}\{e^{-i\omega_{\rm rf}t}\tilde{V}\} = V\cos(\omega_{\rm rf}t + \theta_V), \tag{A9}$$

where we wrote $\tilde{V} = Ve^{-i\theta_V}$ for the total voltage phasor and, based on the *RLC* circuit model, $\tilde{V}_g = Z(\omega_{\rm rf})I_ge^{-i\theta_g}$.

A test particle with time-of-flight coordinate $\tau$ travels through the cavity at times $t = t_0 + nT_0 + \tau$. The requirement that in Eq. (A9) the synchronous particle ($\tau = 0$) sees the synchronous phase $\psi_s$ defines $t_0 = (\psi_s - \theta_V)/\omega_{\rm rf}$. Inserting $t = t_0 + nT_0 + \tau$ in (A4),

$$\mathcal{V}_b(\tau) = -2I_{\rm avg}R_sF_1\cos\phi_{r1}\cos(\omega_{\rm rf}\tau - \phi_{r1} - \Phi_1), \quad \text{(A10)}$$

and similarly inserting in (A8),

$$\mathcal{V}_g(\tau) = I_gR_{L1}\cos\phi_{r1}\cos(\omega_{\rm rf}\tau + \psi_s - \theta_V - \phi_{r1} + \theta_g), \quad \text{(A11)}$$

which leads to the definition $\psi_{s,g} = \psi_s - \theta_V - \phi_{r1} + \theta_g$ for the generator voltage synchronous phase. In conclusion, with the generator and beam peak voltages defined in (2) and (3) we can write the total main-cavity voltage as

$$V\cos(\omega_{\rm rf}\tau + \psi_s) = V_g\cos(\omega_{\rm rf}\tau + \psi_{s,g}) - V_b\cos(\omega_{\rm rf}\tau - \phi_{r1} - \Phi_1). \quad \text{(A12)}$$

The generator voltage is susceptible to amplitude ($I_g = I_{g0} + \Delta I_g$) or phase ($\theta_g = \theta_{g0} + \Delta\theta_g$) noise. The amplitude perturbation is generally less significant and in this paper is neglected. Since we are not interested in absolute timing, it does no harm to set $\theta_{g0} = 0$.

We are interested in the first-order expansions of $\mathcal{V}_g$ in the combined $\tau$ and $\Delta\theta_g$ (i.e., we regard and neglect $\tau\Delta\theta_g$ as second order) and of $\mathcal{V}_b$ in $(\tau - \Phi_1/\omega_{\rm rf}) = (\tau - \langle\tau\rangle)$ where we made use of Eq. (A6) to represent $\Phi_1$:

$$\mathcal{V}_g(\tau) \simeq V_g\cos\psi_{s,g} - \tau V_g\omega_{\rm rf}\sin\psi_{s,g} - \Delta\theta_gV_g\sin\psi_{s,g}, \quad \text{(A13)}$$

$$\mathcal{V}_b(\tau) \simeq -V_b\cos\phi_{r1} - (\tau - \langle\tau\rangle)V_b\omega_{\rm rf}\sin\phi_{r1}. \quad \text{(A14)}$$

## APPENDIX B: rf CAVITY FUNDAMENTAL-MODE IMPEDANCE

At time $t > 0$, the induced-voltage response of an rf cavity fundamental mode to the passage of a pointlike charge at $t = 0$ is described by the wake function $W(t) = 2\alpha Re^{-\alpha t}[\cos(\bar\omega t) - \frac{\alpha}{\bar\omega}\sin(\bar\omega t)]$, where $\alpha = \omega_r/(2Q)$, $\bar\omega = \sqrt{\omega_r^2 - \alpha^2} = \omega_r\sqrt{1 - 1/(2Q)^2}$, and $\omega_r$ is the resonant frequency; $W(t) = 0$ for $t \le 0$ (causality). The associated impedance $Z(\omega) = \int_{-\infty}^{\infty} dte^{i\omega t}W(t)$ is

$$Z(\omega) = \frac{R}{1 + iQ(\frac{\omega_r}{\omega} - \frac{\omega}{\omega_r})} = R\cos[\phi(\omega)]e^{i\phi(\omega)}, \quad \text{(B1)}$$

with the angle $\phi(\omega)$ defined as

$$\tan\phi(\omega) = Q\left(\frac{\omega}{\omega_r} - \frac{\omega_r}{\omega}\right) \simeq 2Q\frac{\omega - \omega_r}{\omega_r}. \quad \text{(B2)}$$

Note that in the convention adopted here $\phi(\omega)$ is positive for $\omega - \omega_r > 0$. It is understood that the main cavity $R$ and $Q$ should be interpreted as the loaded shunt impedance $R_{L1} = R_{U1}/(1+\beta)$ and quality factor $Q_{L1} = Q_{U1}/(1+\beta)$, where $\beta$ is the coupling factor and $R_{U1}$ and $Q_{U1}$ are the unloaded quantities. For passive HHCs without couplers, there is no ambiguity; if a coupler is present, the loaded $R$ and $Q$ should be used.

We are interested in the Taylor expansion of the effective impedance $\zeta_q(\omega)$ in $\omega$ about the frequency $\pm q\omega_{\rm rf}$ ($q = 1$ for the main cavity and $q = n$ for the HHC):

$$\zeta_q(\omega) \equiv \sum_{p=\pm q} pZ(p\omega_{\rm rf} + \omega) \simeq iqR\,\sin 2\phi_r - \left[\frac{4Q}{\omega_{\rm rf}}R\,\sin(2\phi_r)\cos^2\phi_r\right]\omega - \left[i\frac{2QR\cos^2\phi_r}{q\omega_{\rm rf}^2}[\cos 2\phi_r + 2Q(\sin 2\phi_r + \sin 4\phi_r)]\right]\omega^2 \quad \text{(B3)}$$

where $\phi_r \equiv \phi(\omega = q\omega_{\rm rf})$, with

$$\tan\phi_r \simeq 2Q\frac{q\omega_{\rm rf} - \omega_r}{\omega_r}, \quad \text{(B4)}$$

is the detuning angle. In the cases studied in this paper, the second-order term is small in the range of interest and can be neglected. Through first order, we write the effective total impedance for the combined main cavity and HHC as $\zeta(\omega) \simeq \zeta(0) + \zeta'(0)\omega$ with $\zeta(0) = \zeta_1(0) + \zeta_n(0)$, $\zeta'(0) = \zeta_1'(0) + \zeta_n'(0)$, and

$$\zeta_1(0) = iR_{L1}\sin 2\phi_{r1}, \quad \text{(B5)}$$

$$\zeta_n(0) = inR_n\sin 2\phi_{rn}, \quad \text{(B6)}$$

$$\zeta_1'(0) = -(4R_{L1}Q_{L1}/\omega_{\rm rf})\sin 2\phi_{r1}\cos^2\phi_{r1}, \quad \text{(B7)}$$

$$\zeta_n'(0) = -(4R_nQ_n/\omega_{\rm rf})\sin 2\phi_{rn}\cos^2\phi_{rn}. \quad \text{(B8)}$$

## APPENDIX C: DERIVATION OF THE RESPONSE FUNCTION FROM THE SOLUTION OF THE LINEAR VLASOV EQUATION

The prevalent method to solve the linearized Vlasov equation involves the azimuthal/radial mode decomposition $f_1(\varphi, J; \omega) = \sum_{m=-\infty}^{\infty} R_m(J;\omega)e^{im\varphi}$. Written in terms of the scaled current parameter $\hat I = e\omega_{\rm rf}I_{\rm avg}/E_0T_0$ and derivative of the bunch equilibrium $f_0' = \partial f_0/\partial J$, Eq. (24) becomes [19,27]

$$(\omega + i|m|\gamma_d - m\omega_s)R_m + 2\pi i m\hat{I} f_0' \sum_{p=-\infty}^{\infty} \frac{Z(p\omega_{\rm rf}+\omega)}{p\omega_{\rm rf}^2} H^*_{m,p}(J) \times \sum_{m'=-\infty}^{\infty} \int_0^{\infty} dJ' R_{m'}(J') H_{m',p}(J') = \text{rhs}, \tag{C1}$$

where the term $i|m|\gamma_d$, with $\gamma_d \equiv \tau_d^{-1} > 0$, is meant to capture the effect of radiation damping [37] and $H_{m,p}(J) = (2\pi)^{-1}\int_0^{2\pi} e^{im\varphi + ip\omega_{\rm rf} r\cos\varphi} d\varphi = i^m J_m(p\omega_{\rm rf} r)$, $J_m$ being the Bessel function. The rhs of (C1) has the form

$$\text{rhs} = if_0' \int_0^{2\pi} d\varphi e^{-im\varphi} \frac{\partial \mathcal{H}_g}{\partial \varphi} = i\Delta\tilde{\Theta}_g(\omega) f_0' \frac{r(J)}{2\pi} \times \int_0^{2\pi} d\varphi e^{-im\varphi} \sin\varphi = \delta_{1|m|}\text{sign}(m)\Delta\tilde{\Theta}_g(\omega) f_0' \frac{r(J)}{2}, \tag{C2}$$

where $\Delta\tilde{\Theta}_g(\omega) \equiv \omega_{c1}^2 \Delta\tilde{\theta}_g(\omega)/(\omega_{\rm rf}\alpha_c)$ is the normalized generator phase error. We proceed by assuming the dipole approximation and retaining only the terms $m = \pm 1$ in the azimuthal-mode expansion, which is sensible as the driving term (C2) is dipolar in nature. However, as discussed in Sec. V, the quadrupole mode could be driven indirectly by this excitation if a strong dipole/quadrupole coupling were present; in that case, the effect would not be captured in the dipole approximation.

Having introduced the short hand $Z_p \equiv Z(p\omega_{\rm rf}+\omega) = Z^{(1)}(p\omega_{\rm rf}+\omega) + Z^{(n)}(p\omega_{\rm rf}+\omega)$ for the total impedance, $J^{(p)}_{|m|} = J_{|m|}(p\omega_{\rm rf} r)$ for the relevant Bessel function and used $J_{-m}(x) = -J_m(x)$, the left side of Eq. (C1) can be cast in the form ($m = \pm 1$)

$$(\omega + i\gamma_d - m\omega_s)R_m + 2\pi i^m \hat{I} \frac{f_0'}{\omega_{\rm rf}^2} \sum_p pZ_p \frac{J_1^{(p)}}{p} \left[ \int_0^{\infty} dJ' R_1 \frac{J_1^{(p)}}{p} + \int_0^{\infty} dJ' R_{-1} \frac{J_1^{(p)}}{p} \right] = \text{rhs}. \tag{C3}$$

With the further definition $r_m^p = \int_0^{\infty} dJ R_m J_1^{(p)}/p$, and exploiting the assumption that the main and harmonic cavity fundamental-mode impedances are narrow band about the fundamental $\omega_{\rm rf}$ and higher $n\omega_{\rm rf}$ harmonic, respectively, we split the impedance sum into two separate sums:

$$\sum_p pZ_p \frac{J_1^{(p)}}{p}[r_1^p + r_{-1}^p] \simeq \sum_{p=\pm 1} pZ_p^{(1)} \frac{J_1^{(p)}}{p}[r_1^p + r_{-1}^p] + \sum_{p=\pm n} pZ_p^{(n)} \frac{J_1^{(p)}}{p}[r_1^p + r_{-1}^p]. \tag{C4}$$

Observing that $J_1(-px) = -J_1(px)$ and therefore $J_1^{(p)}/p = J_1^{(|p|)}/|p|$ and $r_m^{-p} = r_m^p$, the two terms on the rhs of (C4) read $(Z_1^{(1)} - Z_{-1}^{(1)}) r^1 J_1^{(1)}$ and $n(Z_n^{(n)} - Z_{-n}^{(n)}) r^n J_1^{(n)}/n$, respectively, having introduced $r^1 \equiv r_1^1 + r_{-1}^1$ and $r^n \equiv r_1^n + r_{-1}^n$. With this result and the further definition $\zeta_q \equiv q(Z_q^{(q)} - Z_{-q}^{(q)})$, where $q = 1$ or $n$, we can write (C3) as

$$(\omega + i\gamma_d - m\omega_s)R_m + 2\pi i^m \frac{\hat{I}}{\omega_{\rm rf}^2} f_0' \left[ \zeta_1 J_1^{(1)} r^1 + \zeta_n \frac{J_1^{(n)}}{n} r^n \right] = m\Delta\tilde{\Theta}_g f_0' \frac{r}{2}. \tag{C5}$$

Next, multiply the above equation by $J_1^{(q)}/q$, divide by $(\omega + i\gamma_d - m\omega_s)$, integrate over the action $J$

$$r_m^q + 2\pi i^m \frac{\hat{I}}{\omega_{\rm rf}^2} \left[ \frac{\zeta_1 r^1}{q} \int \frac{f_0' J_1^{(1)} J_1^{(q)} dJ}{\omega + i\gamma_d - m\omega_s} + \frac{\zeta_n r^n}{nq} \int \frac{f_0' J_1^{(n)} J_1^{(q)} dJ}{\omega + i\gamma_d - m\omega_s} \right] = \frac{m\Delta\tilde{\Theta}_g}{q} \int \frac{(r/2) f_0' J_1^{(q)} dJ}{\omega + i\gamma_d - m\omega_s} \tag{C6}$$

and introduce the functions

$$G_m^{p,q}(\omega) \equiv \frac{2\pi}{\omega_{\rm rf}^2 pq} \int dJ \frac{f_0' J_1^{(p)} J_1^{(q)}}{\omega + i\gamma_d - m\omega_s}, \tag{C7}$$

$$D_m^q(\omega) \equiv \frac{2\pi}{\omega_{\rm rf}^2 q} \int dJ \frac{(r/2) f_0' J_1^{(q)}}{\omega + i\gamma_d - m\omega_s}, \tag{C8}$$

to write (C6) as

$$r_m^q + i^m \hat{I}[\zeta_1 r^1 G_m^{1,q} + \zeta_n r^n G_m^{n,q}] = m\Delta\tilde{\Theta}_g \frac{\omega_{\rm rf}^2}{2\pi} D_m^q. \tag{C9}$$

More explicitly, for $m = \pm 1$, the above equation translates into

$$r_1^q + i\hat{I}[\zeta_1 r^1 G_1^{1,q} + \zeta_n r^n G_1^{n,q}] = \Delta\tilde{\Theta}_g \frac{\omega_{\rm rf}^2}{2\pi} D_1^q, \tag{C10}$$

$$r_{-1}^q - i\hat{I}[\zeta_1 r^1 G_{-1}^{1,q} + \zeta_n r^n G_{-1}^{n,q}] = -\Delta\tilde{\Theta}_g \frac{\omega_{\rm rf}^2}{2\pi} D_{-1}^q. \tag{C11}$$

Upon taking the sum of the two equations above, first with $q = 1$ and then $q = n$, we obtain the system

$$\begin{bmatrix} 1+i\hat{I}\zeta_1 G_{1,1} & i\hat{I}\zeta_n G_{n,1} \\ i\hat{I}\zeta_1 G_{n,1} & 1+i\hat{I}\zeta_n G_{n,n} \end{bmatrix} \begin{bmatrix} r^1 \\ r^n \end{bmatrix} = \Delta\tilde{\Theta}_g \frac{\omega_{\rm rf}^2}{2\pi} \begin{bmatrix} D_1 \\ D_n \end{bmatrix}, \tag{C12}$$

having introduced the following additional functions:

$$G_{p,q}(\omega) \equiv G_1^{p,q} - G_{-1}^{p,q} = \frac{4\pi}{\omega_{\rm rf}^2 pq} \int dJ f_0' \frac{\omega_s(J) J_1(p\omega_{\rm rf} r) J_1(q\omega_{\rm rf} r)}{\omega^2 + 2i\gamma_d \omega - \omega_s^2(J)}, \tag{C13}$$

and

$$D_q(\omega) \equiv D_1^q - D_{-1}^q = \frac{4\pi}{\omega_{\rm rf}^2 q} \int dJ f_0' \frac{(r/2)\omega_s(J) J_1(q\omega_{\rm rf} r)}{\omega^2 + 2i\gamma_d \omega - \omega_s^2(J)}. \tag{C14}$$

In Eqs. (C13) and (C14), we neglected $\gamma_d^2$ compared to $\omega_s^2$. The approximate solution of (C12)

$$r^1 = \frac{\omega_{\rm rf}^2}{2\pi} \Delta\tilde{\Theta}_g \frac{D_1 - i\hat{I}\zeta_n (D_n G_{1,n} - D_1 G_{n,n})}{\det} \simeq \frac{\omega_{\rm rf}^2}{2\pi} \Delta\tilde{\Theta}_g \frac{D_1}{\det}, \tag{C15}$$

$$r^n = \frac{\omega_{\rm rf}^2}{2\pi} \Delta\tilde{\Theta}_g \frac{D_n + i\hat{I}\zeta_1 (D_n G_{1,1} - D_1 G_{1,n})}{\det} \simeq \frac{\omega_{\rm rf}^2}{2\pi} \Delta\tilde{\Theta}_g \frac{D_n}{\det}, \tag{C16}$$

where

$$\det \equiv 1 + i\hat{I}(G_{1,1}\zeta_1 + G_{n,n}\zeta_n) + \hat{I}^2 [G_{1,1} G_{n,n} - (G_{1,n})^2] \zeta_1 \zeta_n \tag{C17}$$

is inserted in (C5) to find

$$(\omega + i\gamma_d - \omega_s) R_{\pm 1} \simeq \Delta\tilde{\Theta}_g f_0' \frac{r}{2} \left[\frac{\pm 1}{\det}\right]. \tag{C18}$$

The approximation in (C18) comes from neglecting terms proportional to $\Delta\tilde{\Theta}_g \hat{I}$ and $\Delta\tilde{\Theta}_g \hat{I}^2$. Equation (C18) leads to

$$R_1 + R_{-1} = f_0' \frac{r\omega_s}{\omega^2 + 2i\gamma_d \omega - \omega_s^2} \frac{\Delta\tilde{\Theta}_g(\omega)}{\det}, \tag{C19}$$

and finally

$$\langle \tau \rangle = \pi \int dJ (R_1 + R_{-1}) r = \frac{\Delta\tilde{\Theta}_g(\omega) S_1(\omega)}{\det}, \tag{C20}$$

with

$$S_1(\omega) = \pi \int dJ f_0' \frac{r^2 \omega_s}{\omega^2 + 2i\gamma_d \omega - \omega_s^2}. \tag{C21}$$

For short bunches, the following approximations typically hold: $S_1 \simeq G_{1,1} \simeq \omega_{\rm rf} D_1$. On the assumption that this is true, $\langle \tau \rangle \equiv \Delta\tilde{\varphi}_b / \omega_{\rm rf} \simeq \Delta\tilde{\Theta}_g(\omega) G_{1,1} / \det$, and finally the response function reads

$$\frac{\Delta\tilde{\varphi}_b}{\Delta\tilde{\theta}_g} \simeq \frac{\omega_{c1}^2}{\alpha_c} \frac{G_{1,1}}{\det}. \tag{C22}$$


[1] A. Hofmann and S. Myers, Beam dynamics in a double RF system, CERN Report No. ISR-TH-RF/80-26, 1980.

[2] R. Biscardi, S. L. Kramer, and G. Ramirez, Bunch length control in the NSLS VUV ring, Nucl. Instrum. Methods Phys. Res., Sect. A **366**, 26 (1995).

[3] M. Georgsson, Å. Andersson, and M. Eriksson, Landau cavities at MAX-II, Nucl. Instrum. Methods Phys. Res., Sect. A **416**, 465 (1998).

[4] J. M. Byrd, S. De Santis, M. Georgsson, G. Stover, J. D. Fox, and D. Teytelman, Commissioning of a higher harmonic rf system for the Advanced Light Source, Nucl. Instrum. Methods Phys. Res., Sect. A **455**, 271 (2000).

[5] D. Alesini *et al.*, The DAFNE 3rd harmonic cavity, in *Proceedings of the 19th Particle Accelerator Conference Chicago, IL, 2001* (IEEE, Piscataway, NJ, 2001), p. 885.

[6] W. Anders and P. Kuske, HOM damped NC passive harmonic cavities at BESSY, in *Proceedings of the 20th Particle Accelerator Conference, PAC-2003, Portland, OR, 2003* (IEEE, New York, 2003), p. 1186.

[7] M. Pedrozzi *et al.*, SLS operational performance with third harmonic superconducting system, in *Proceedings of the 11th Workshop on rf Superconductivity, Lübeck, Germany,* (2003), https://accelconf.web.cern.ch/SRF2003/papers/mop25.pdf.

[8] M. Svandrlik *et al.*, Performance of the 3rd harmonic superconducting cavity at ELLETRA, in *Proceedings of the 11th Workshop on rf Superconductivity, Lübeck, Germany,* (2003), https://accelconf.web.cern.ch/SRF2003/papers/mop27.pdf.

[9] M. P. Kelly *et al.*, Superconducting harmonic cavity for the Advanced Photon Source Upgrade, in *Proceedings of the 6th International Particle Accelerator Conference, IPAC-2015, Richmond, VA, 2015* (JACoW, Geneva, Switzerland, 2015), WEPTY005.

[10] Y. H. Chin, Longitudinal stability limit for electron bunches in a double rf system, Nucl. Instrum. Methods Phys. Res., Sect. A **215**, 501 (1983).

[11] S. Krinksy and J. M. Wang, Longitudinal instabilities of bunched beams subject to a non-harmonic rf potential, Part. Accel. **17**, 109 (1985).

[12] J. M. Wang, Modes of storage ring coherent instabilities, AIP Conf. Proc. **153**, 697 (1987).

[13] T.-S. F. Wang, Bunched-beam longitudinal mode-coupling and Robinson-type instabilities, Part. Accel. **34**, 105 (1990).

[14] B. Bosh and C. Hsue, Suppression of longitudinal couple-bunch instabilities by a passive higher order harmonic cavities, Part. Accel. **42**, 81 (1993).
[15] M. Migliorati, L. Palumbo, and M. Zobov, Bunch length control in DAFNE by a higher harmonic cavity, Nucl. Instrum. Methods Phys. Res., Sect. A **354**, 215 (1995).
[16] R. A. Bosh, K. J. Kleman, and J. J. Bisognano, Phys. Rev. ST Accel. Beams **4**, 074401 (2001).
[17] F. J. Cullinan, R. Nagaoka, G. Skripka, and P. F. Tavares, Transverse coupled-bunch instability thresholds in the presence of a harmonic-cavity-flattened rf potential, Phys. Rev. Accel. Beams **19**, 124401 (2016).
[18] M. Venturini, Harmonic cavities and the transverse mode-coupling instability driven by a resistive wall, Phys. Rev. Accel. Beams **21**, 024402 (2018).
[19] M. Venturini, Passive higher-harmonic rf cavities with general settings and multibunch instabilities in electron storage rings, Phys. Rev. Accel. Beams **21**, 114404 (2018).
[20] F. J. Cullinan, Å. Andersson, and P. F. Tavares, Harmonic-cavity stabilization of longitudinal coupled-bunch instabilities with a nonuniform fill, Phys. Rev. Accel. Beams **23**, 074402 (2020).
[21] R. Lindberg, Theory of longitudinal coupled-bunch instabilities in a storage ring for arbitrary rf potentials, Phys. Rev. Accel. Beams **21**, 124402 (2018).
[22] E. N. Shaposhnikova, CERN Report No. SL-94-19-RF, 1994.
[23] N. Towne, Longitudinal simulations and measurements of stretched bunches, Phys. Rev. ST Accel. Beams **4**, 114401 (2001).
[24] R. A. Bosh and J. J. Kleman, Effect of dipole-quadrupole Robinson mode coupling upon the beam response to radio-frequency phase noise, Phys. Rev. ST Accel. Beams **9**, 094401 (2006).
[25] F. Pedersen, Beam loading effects in the CERN PS Booster, IEEE Trans. Nucl. Sci. **22**, 1906 (1975).
[26] J. Byrd, Effects of phase noise in heavily beam-loaded storage rings, in *Proceedings of the 18th Particle Accelerator Conference, New York, 1999* (IEEE, New York, 1999), p. 1806.
[27] K. Ng, *Physics of Intensity Dependent Beam Instabilities* (World Scientific, Singapore, 2006).
[28] P. Wilson, Transient beam loading in electron-positron storage rings, Report No. CERN-ISR-TH/89-23, 1978; P. Wilson, High energy electron linacs: Applications to storage ring rf systems and linear colliders, Report No. SLAC-PUB-2884, 1991.
[29] M. Sands, Beam-cavity interaction I. Basic considerations, Laboratoire de l'Accelerateur Lineaire, Orsay, Technical Report No. LAL-RT-2-76, 1976, https://lib-extopc.kek.jp/preprints/PDF/1977/7702/7702218.pdf.
[30] S. Heifets and D. Teytelman, Effect of coupled-bunch modes on the longitudinal feedback system, Phys. Rev. ST Accel. Beams **10**, 012804 (2007).
[31] S. Koscielniak, A general theory of beam loading, Part. Accel. **31**, 205 (1990); , Analytic criteria for stability of beam-loaded radio-frequency systems, Part. Accel. **48**, 135 (1994).
[32] P. F. Tavares, A. Andersson, A. Hansson, and J. Breulin, Equilibrium bunch density distribution with passive harmonic cavities in a storage ring, Phys. Rev. Accel. Beams **17**, 064401 (2014).
[33] C. Steier *et al.*, Status of the conceptual design of ALS-U, in *Proceedings of the 9th International Particle Accelerator Conference, IPAC-2018, Vancouver, BC, Canada, 2018* (JACoW, Geneva, Switzerland, 2018), pp. 4134–4137, 10.18429/JACoW-IPAC2018-THPMF036.
[34] J. Byrd, De Santis, J. Jacob, and V. Serriere, Transient beam loading effects in harmonic rf systems for light sources, Phys. Rev. ST Accel. Beams, **5**, 092001 (2002).
[35] M. Borland, ELEGANT: A flexible SDDS-compliant code for accelerator simulation, Report No. APS LS-287, 2000.
[36] T. Luo *et al.*, Design progress of ALS-U 3rd-harmonic cavity, in *Proceedings of the 12th International Particle Accelerator Conference, IPAC-2021, Campinas, SP, Brazil, 2021* (JACoW, Geneva, Switzerland, 2021), p. 1482.
[37] Y. Suzuki, Theory of longitudinal bunched-beam instabilities based on the Fokker-Planck equation, Part. Accel. **14**, 91 (1983).